Contribution of satellite gravimetry to understanding seismic source processes of the 2011 Tohoku-Oki earthquake

Shin-Chan Han,[1,2] Jeanne Sauber,[1] and Riccardo Riva[3]

Received 11 October 2011; revised 16 November 2011; accepted 19 November 2011; published 29 December 2011.

[1] The 2011 great Tohoku-Oki earthquake, apart from shaking the ground, perturbed the motions of satellites orbiting some hundreds km away above the ground, such as GRACE, due to coseismic change in the gravity field. Significant changes in inter-satellite distance were observed after the earthquake. These unconventional satellite measurements were inverted to examine the earthquake source processes from a radically different perspective that complements the analyses of seismic and geodetic ground recordings. We found the 'average' slip located up-dip of the hypocenter but within the lower crust, as characterized by a limited range of bulk and shear moduli. The GRACE data constrained a group of earthquake source parameters that yield increasing dip (7–16° ± 2°) and, simultaneously, decreasing moment magnitude (9.17–9.02 ± 0.04) with increasing source depth (15–24 km). The GRACE solution includes the cumulative moment released over a month and demonstrates a unique view of the long-wavelength gravimetric response to all mass redistribution processes associated with the dynamic rupture and short-term postseismic mechanisms to improve our understanding of the physics of megathrusts. **Citation:** Han, S.-C., J. Sauber, and R. Riva (2011), Contribution of satellite gravimetry to understanding seismic source processes of the 2011 Tohoku-Oki earthquake, *Geophys. Res. Lett.*, *38*, L24312, doi:10.1029/2011GL049975.

1. Introduction

[2] The great Tohoku-Oki earthquake on March 11, 2011 shook the Honshu island in Japan radiating seismic energy (M_w 9.0–9.1), deformed the surface near the epicenter permanently up to 10–30 meters horizontally and a few meters vertically, and generated a devastating tsunami of tens of meters in height [*Ozawa et al.*, 2011; *Sato et al.*, 2011; *Simons et al.*, 2011]. Various geophysical signals of ground, seafloor, and sea-surface motions were measured by seismometers, GPS, seafloor transponders, and tsunami gauges, and these measurements have been exploited to understand the rupture dynamics and spatial extent of slip [*Lay et al.*, 2011; *Pollitz et al.*, 2011; *Simons et al.*, 2011]. The analyses of ground-based observations of the earthquake consistently indicate a compact source with slip of 30–60 m, allowing a single double-couple source to explain long-period seismic radiation data [*Shao et al.*, 2011]. However, the 'average' slip appears down-dip [*Ammon et al.*, 2011; *Ozawa et al.*, 2011; *Simons et al.*, 2011], up-dip [*Pollitz et al.*, 2011; *Shao et al.*, 2011] of the hypocenter (~24 km deep), or even shallower near trench [*Lay et al.*, 2011], due to the limited sensitivity and coverage of seismic and geodetic observations to mapping the rupture processes [*Lay et al.*, 2011; *Pollitz et al.*, 2011]. Although the fault plane was fixed to approximate the dip of the top surface of the downgoing slab constrained by seismic reflection data [*Miura et al.*, 2005], the estimated moment of this earthquake ranges from 3.9 to 5.8 × 10^{22} N-m, depending on the analysis technique, source depth, data weighting, the presumed Earth structure as well as additional parameters. The inverted slip distribution and magnitude among numerous models still differ substantially, although they produce consistent fits to different kinds of traditional ground measurements [*Pollitz et al.*, 2011].

[3] Earthquakes, apart from triggering seismic waves and causing surface displacement, redistribute mass within the Earth and thus change the gravitational field. The coseismic gravity change is due to deformation inside of the Earth as well as on the surface (including the interaction with the ocean) [*Han et al.*, 2006, 2010; *De Linage et al.*, 2009; *Melini et al.*, 2010; *Broerse et al.*, 2011; *Cambiotti et al.*, 2011]. While the surface displacement is accessible from other geodetic techniques such as GPS and InSAR, the interior deformation, that includes changes in intrinsic density (or volume) and vertical deformation of the discontinuities in density stratification of the interior, can be addressed best through gravimetric observations [*Okubo*, 1992; *Pollitz*, 1997]. The coseismic changes in the gravitational field are dependent on the seismic source depth, focal mechanism (strike, dip, and rake) and physical properties of the Earth as well as the earthquake magnitude (Figures S1 and S2 in the auxiliary material).[1] For example, a seismic source with smaller moment may produce larger gravity change than the one with larger moment depending on these parameters, especially, source depth and fault dip (Figures S3 and S4). A deeper seismic source with higher dip and a shallower source with lower dip may produce similar gravity change (Figure S5).

2. Measurements of Coseismic Changes in GRACE Inter-satellite Ranging Data

[4] The coseismic gravitational potential changes, in turn, influence the orbital motion of spacecraft [*Han et al.*, 2010]. The inter-satellite distance changes (i.e., range-rate) between two GRACE satellites orbiting at 480 km altitude have been

[1]Planetary Geodynamics Laboratory, NASA Goddard Space Flight Center, Greenbelt, Maryland, USA.
[2]Also at Joint Center for Earth Systems Technology, University of Maryland, Baltimore County, Baltimore, Maryland, USA.
[3]Faculty of Aerospace Engineering, Delft University of Technology, Delft, Netherlands.

Copyright 2011 by the American Geophysical Union.
0094-8276/11/2011GL049975

[1]Auxiliary material data sets are available at ftp://ftp.agu.org/apend/gl/2011gl049975. Other auxiliary material files are in the HTML.

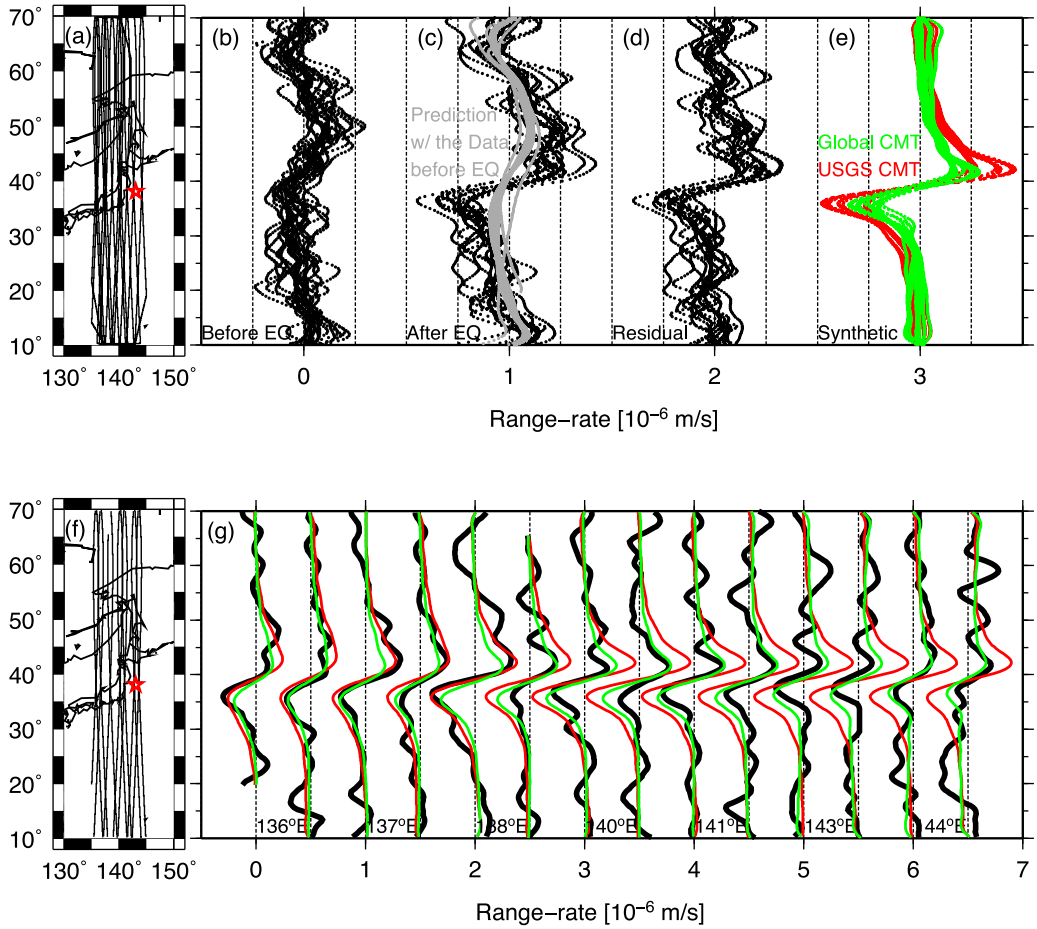

Figure 1. GRACE measurements of range-rate change before and after the earthquake. (a) The satellite ground tracks near the epicenter from February 11 to March 10, 2011 (before the earthquake). (b) GRACE observations before the earthquake. (c) GRACE observations from March 11 to March 31, 2011 (after the earthquake). The gray lines indicate the predicted non-earthquake effect for the data after the earthquake. They were determined from the data immediately before the earthquake. (d) The residual GRACE data after removing the non-earthquake signals. (e) The synthetic range-rate responses from two seismic CMT solutions. (f) The satellite ground tracks during March 11 to 31, 2011 corresponding to the data shown in Figure 1c. (g) The individual passes of the GRACE observations and seismic model synthetics of coseismic range-rate change (see Figures S4a and S4b for the corresponding synthetic surface gravity change). A pair of passes at each mean longitude (shown at the bottom of Figure 1g) is from ascending and descending tracks with a time difference of 12 hours. For clarity in the plot, only two weeks of the GRACE data west of the epicenter were shown; data east of the epicenter are shown in Figure S6 in the auxiliary material.

measured with the onboard K-Band Ranging (KBR) instrument. These are the fundamental observations used to construct monthly time-series of global gravity fields delivered by the mission since 2002 [*Tapley et al.*, 2004]. We examined these range-rate measurements near the epicenter before and after the earthquake (the satellite ground tracks west of the epicenter are shown in Figures 1a and 1f, respectively). When four weeks of pre-earthquake GRACE measurements (Figure 1b) and the two weeks after the earthquake (Figure 1c) are compared, significant changes were observed between the latitudes 35–43°N. To retain only the changes by the earthquake, we removed nuisance 'mass variation' signals that coexist in the GRACE measurements such as those due to fluctuations in the ocean, atmosphere, snow level and land water storage. The reference global mass distribution from these various background signals was estimated from one month worth of the GRACE data immediately before the earthquake (in terms of 'usual' spherical harmonic coefficients). This was used to compute the effect of non-earthquake signals in the data after the earthquake (shown as gray in Figure 1c), assuming no significant changes occurred from non-earthquake sources during one month.

[5] The residuals, defined by the difference between the actual observations and the predicted non-earthquake signals, reflect the coseismic changes in range-rate (Figure 1d). The corresponding synthetic range-rate changes were computed (see auxiliary material), using global centroid moment tensor (GCMT) [*Nettles et al.*, 2011] and USGS CMT [*U.S. Geological Survey*, 2011] solutions as examples. The difference between two seismic solutions is large with the maximum of $\sim 0.2 \times 10^{-6}$ m/s (Figure 1e) and, when

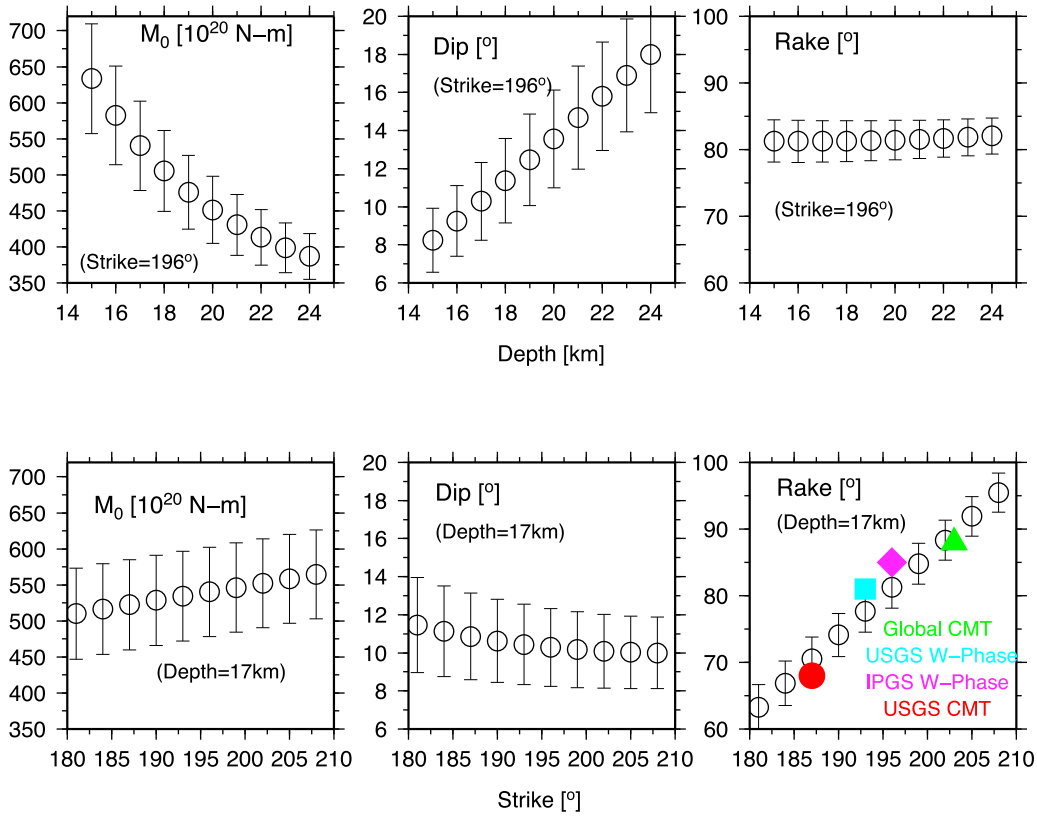

Figure 2. GRACE estimates of the earthquake source parameters from inversion of one month of range-rate data after the earthquake. (top) GRACE solutions of scalar moment, dip, and rake with a fixed fault strike of 196° at various depths within the lower crust for 'slip' centroid (i.e., point dislocation). The moment and dip estimates change monotonically with depth, while the rake estimates are relatively constant regardless of depth. (bottom) GRACE solutions with variable strike at a fixed centroid depth of 17 km. A change in strike is compensated by the rake parameter without causing much change in moment and dip parameters. The monotonic relationship between rake and strike is also found from various seismic CMT solutions.

compared with the measurements, USGS CMT was found to overestimate the coseismic range-rate (i.e., gravity) changes. This demonstrates how the gravity response from seismic source is not simply proportional to the size of the earthquake, because the scalar moment of USGS CMT is 20% smaller than that of GCMT. Finally, the largest range-rate changes from GRACE were observed west of the epicenter implying the location where coseismic gravity change is substantial (Figures 1g and S6 presenting the GRACE data east of the epicenter).

[6] Three seismic CMT solutions [*Duputel et al.*, 2011; *Hayes*, 2011; *Nettles et al.*, 2011] with the centroid moment sources in the lower crust (15–24 km depth), as defined by PREM [*Dziewonski and Anderson*, 1981], agree with the GRACE range-rate measurements yielding more than 65% of variance reduction (VR) (Figure S7a). However, USGS CMT specified with the source at 10 km depth within the upper crust gives distinctly poorer agreement with VR less than 40%. Since the centroid depth is not generally well-constrained by long-period seismic data [*Kanamori and Given*, 1981], we tested these CMT solutions within a depth range of 3–40 km. We found that the synthetic gravity change from all CMT solutions may be reconciled with the GRACE range-rate observations, if the source depth is adapted to be within the lower crust characterized by a certain range of elastic parameters such as compressional and shear moduli and density (Figure S7). An earthquake source at shallower depth may cause larger coseismic gravity change than the same source at deeper (and more rigid) layer, because the ambient material of the shallower layer is more deformable in volume and shape.

3. Inversion for Earthquake Source Parameters

[7] The GRACE measurements open a new opportunity to examine the earthquake source through gravitational potential normal modes (involving spheroidal modes). Analogous to inversion of long-period seismic waveform data through spheroidal and toroidal displacement modes in the elasto-gravitational eigenproblem [*Gilbert and Backus*, 1968], we have estimated the earthquake double-couple source parameters from the GRACE range-rate data with a presumed location of slip. By fixing its latitude, longitude, and depth, the gravity response functions (i.e., Green's functions) were computed *a priori*. The linear observational models of the GRACE measurements were, then, constructed with respect to the moment tensor elements indicating orientation (strike, dip, and rake) and size (moment) of the fault dislocation.

[8] In inversion of the GRACE inter-satellite range-rate measurements, we solved simultaneously for scalar moment M_0, dip δ, and rake λ parameters with a fixed fault strike and variable depths, and alternatively, with a fixed depth and variable fault strikes (Figures 2, top and 2, bottom, respectively). In the former case, the estimate of scalar moment

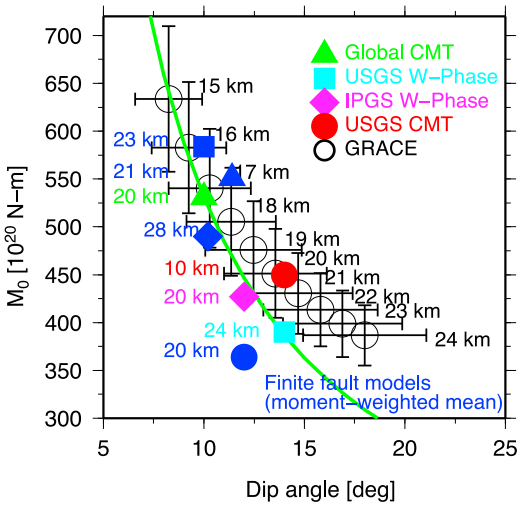

Figure 3. Scalar moment M_0 versus fault dip δ for variable depth parameters, for GRACE CMT, seismic CMT solutions, and moment-weighted averages of various finite fault models. The GRACE estimates of M_0 and δ at each depth (shown on the right of the symbol) are presented with the respective formal errors (open black circles with error bars). Various seismic CMT solutions are given at different depths (color symbols with depths shown on the left). Multiple CMT's in each finite fault model were averaged with the weights specified by moment (or by slip, if moment is not available) to obtain an approximate point (centroid) representation (blue square [*Shao et al.*, 2011], blue triangle [*Simons et al.*, 2011], blue diamond [*Hayes*, 2011], blue circle [*Ammon et al.*, 2011]). The scalar moment estimate from seismic methods, for example from global CMT solution, varies with filter parameters and centroid depths at the range of M_w 9.03 to 9.16 or, equivalently, 4.0 to 6.0 $\times$ 10^{22} N-m [*Nettles et al.*, 2011]. The green line is the 'isoline' delineating the same value of M_0 sin 2δ as the one of GCMT. Due to the moment-dip 'trade-off' in the long-period seismic data analysis, M_0 sin 2δ is better constrained than each of M_0 and δ. Except for the USGS CMT and a point approximate of two finite fault models [*Ammon et al.*, 2011; *Hayes*, 2011], others are consistent in terms of M_0 sin 2δ and depth. Although all of the GRACE solutions at depths of 15 to 24 km fit the range-rate measurements equally well (Figure S8), the GRACE solutions at shallower depths (15–19 km) are most consistent with the majority of the seismic results at depths greater than 20 km.

decreases from 6.3 to 3.8 $\times$ 10^{22} N-m (M_w 9.1 to 9.0) when depth varies from 15 to 24 km with formal error as large as $\sim$10% of the estimate. At the same time, the dip estimate increases with depth from 8 to 18° $\pm$ $\sim$2°. In contrast, the rake estimate of 82° $\pm$ 3° is constant, regardless of which depth is used. The solutions at other depths (shallower than 15 km or deeper than 24 km) could be ruled out because they produce considerably less agreement (smaller VR) with the measurements. When depth is fixed and strike varies, the inversion shows opposite trends. Namely, the rake estimate monotonically increases with increasing strike (which also can be inferred from the geometry of the fault), while the scalar moment and dip estimates are relatively constant. Any error in the strike estimate will be compensated with the rake estimate, and, fortunately, less likely leaks into the estimates of moment and dip that are usually not well-constrained, albeit more crucial for assessing tsunami and postseismic processes. The trade-off between strike and rake could also be found among various seismic CMT solutions. However, monotonic changes in dip or moment estimates with depth are not found in, for example, global CMT analyses of long-period seismic waves for this earthquake [*Nettles et al.*, 2011].

[9] We adopted the GRACE solutions estimated with a fault strike of 196° and compared with seismic CMT solutions (Figure 3). The long-period seismic data analysis for shallow earthquakes is confronted with the trade-off between scalar moment and dip [*Kanamori and Given*, 1981], which makes various seismic CMT solutions more consistent when compared in terms of M_0 sin 2δ, instead of M_0 and δ individually. The GRACE solutions of M_0 and δ at lower depths (15–20 km) are particularly in accordance with the seismic CMT solutions in terms of M_0 sin 2δ. However, the GRACE depth, indicative of where most of the moment was released, is shallower than the depths of seismic CMT solutions and of the hypocenter (24–32 km). It supports the idea of concentrated slip up-dip of the hypocenter, which is also found from other analysis based on GPS and long period seismic data [*Lay et al.*, 2011; *Pollitz et al.*, 2011; *Shao et al.*, 2011]. The point source approximation (centroid) of various finite fault models [*Ammon et al.*, 2011; *Hayes*, 2011; *Shao et al.*, 2011; *Simons et al.*, 2011], obtained by taking a weighted mean of multiple moments (or slips) in each model, were also compared. In general, the centroids of these models are consistent with seismic CMT solutions, however, lower magnitude [*Ammon et al.*, 2011] or deeper centroid [*Hayes*, 2011] is also found.

4. Discussion

[10] The surface gravity change computed from one of our preferred GRACE solutions (M_0 5.4 $\times$ 10^{22} N-m, dip 10.5°, rake 82°, strike 196°, depth 17 km) found the primary gravity change in the onshore region with -8 μGal or greater in magnitude extending over 700 km and a secondary anomaly of 4 μGal or less offshore (Figure 4a). The maximum gravity difference among the GRACE solutions at various depths in the lower crust is about $\pm$1.5 μGal at the spatial resolution of 500 km. All three recent great earthquakes including the 2004 Sumatra-Andaman islands and the 2010 Maule, Chile caused consistently the larger negative gravity onland and the smaller positive gravity offshore [*Han et al.*, 2006, 2010; *De Linage et al.*, 2009; *Heki and Matsuo*, 2010; *Matsuo and Heki*, 2011]. This is the characteristic spatial pattern of the coseismic gravity change after undersea thrust earthquakes accompanied by crustal dilatation [*Han et al.*, 2006].

[11] The GRACE estimate of coseismic moment may be larger than the seismic estimate because the data over a month were used in the inversion. The analysis of postseismic GPS displacement data predicts 10% of the coseismic moment release ($\sim$4.5 $\times$ 10^{21} N-m) occurred over a month after the main rupture [*Ozawa et al.*, 2011]. The postseismic gravity change would be distinctly different from the coseismic one in its spatial pattern (Figure 4b). The northwest migration of the negative peak is due to the

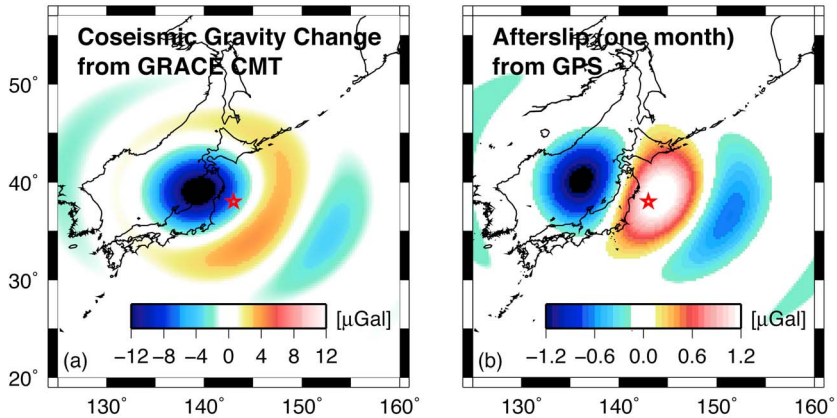

Figure 4. (a) Surface gravity changes computed from the GRACE solution of the earthquake, at a spatial resolution of 500 km (or spherical harmonic degree up to 40). (b) Predicted postseismic gravity changes from the afterslip model for one month, constrained by GPS. The postseismic slip model parameters are described in Figure S9. The GRACE coseismic gravity change includes the cumulative slip over one month. Note the order of magnitude difference in the gravity signal between the coseismic and afterslip models as well as the migration of the peak signal downdip. The effect of isotropic excitation, mostly responsible for a large central negative anomaly in the gravity change, reduces with increasing dislocation depths and the non-isotropic modes (dipole and quadrupole) become more pronounced in the total gravity change (Figures S2 and S3). Therefore, it is anticipated that the negative gravity anomalies onshore is diminished in the postseismic gravity change due to migration of the dislocation toward deeper slab depths in the back-arc region, creating the distinct difference in spatial pattern of the gravity change from coseismic to postseismic period.

location of afterslip downdip from the main shock, while the large ratio of the positive to negative gravity anomalies is due to the slip as it moves into a deeper layer such as the upper mantle. Viscoelastic relaxation may contribute to such postseismic gravity change, as shown to be dominant particularly at a large spatial scale after the 2004 Sumatra-Andaman rupture [*Han et al.*, 2008].

[12] Being sensitive to gravitational normal modes, the GRACE data offered another perspective into the source mechanism and processes associated with the rupture in great earthquakes that complement analysis based on observations of vertical and horizontal surface displacement. This independent view through an alternative physical quantity helps understanding of the earthquake process by untangling the uncertainties in various parameters and by delineating the slip centroid depth in the lower crust. The spatially- and temporally-integrated fault solution such as from GRACE will be beneficial especially to global geodynamic investigations of changes in rotation and figure of the Earth [*Chao and Gross*, 1987]. Continuous observations of gravitational potential changes will be useful to characterize the mechanical and rheological properties of the Earth's interior and the evolving postseismic deformation that may lead to a better understanding of seismic hazard following great earthquakes. The sensitivity of GRACE data to depth and dip indicates the importance of moment distribution as function of depth. A simultaneous inversion of GPS, GRACE, and seismic records for co- and post-seismic slip distribution will give a self-consistent view of this megathrust earthquake and the Earth's response to it. The future GRACE follow-on mission equipped with enhanced instrumentation [*Watkins et al.*, 2011] will allow exploiting gravitational potential data in the analysis of smaller and thus more frequent seismic events.

[13] **Acknowledgments.** This work was supported by NASA Earth Surface and Interior program and GRACE projects. We thank DLR for providing the GRACE telemetry data and JPL for producing the high-quality Level-1B products. We are indebted to Emile Okal for his original suggestion for using gravitational normal mode and its formulation. We thank Fred Pollitz, Richard Gross, Junkee Rhie, Meridith Nettles, Chen Ji, and Nick Schmerr for valuable discussion on earthquake modeling and Scott Luthcke and David Rowlands for helping with GRACE L1B data processing. We thank the reviewers for constructive and thorough comments to improve this manuscript. Finally, we acknowledge the information provided by Group on Earth Observations (GEO) through the GEO geohazards supersite website http://supersites.earthobservations.org/. The GRACE gravity solution in terms of spherical harmonic coefficients is available from AGU website.

[14] The Editor thanks Yoichi Fukuda and an anonymous reviewer for their assistance in evaluating this paper.

References

Ammon, C. J., T. Lay, H. Kanamori, and M. Cleveland (2011), A rupture model of the 2011 off the Pacific coast of Tohoku earthquake, *Earth Planets Space*, *63*, 693–696, doi:10.5047/eps.2011.05.015.

Broerse, D. B. T., L. L. A. Vermeersen, R. E. M. Riva, and W. van der Wal (2011), Ocean contribution to co-seismic crustal deformation and geoid anomalies: Application to the 2004 December 26 Sumatran-Andaman earthquake, *Earth Planet. Sci. Lett.*, *305*, 341–349, doi:10.1016/j.epsl.2011.03.011.

Cambiotti, G., A. Bordoni, R. Sabadini, and L. Colli (2011), GRACE gravity data help constraining seismic models of the 2004 Sumatran earthquake, *J. Geophys. Res.*, *116*, B10403, doi:10.1029/2010JB007848.

Chao, B. F., and R. S. Gross (1987), Changes in the Earth's rotation and low-degree gravitational field induced by earthquakes, *Geophys. J. R. Astron. Soc.*, *91*, 569–596.

De Linage, C., et al. (2009), Separation of coseismic and postseismic gravity changes for the 2004 Sumatra–Andaman earthquake from 4.6 yr of GRACE observations and modelling of the coseismic change by normal-modes summation, *Geophys. J. Int.*, *176*, 695–714, doi:10.1111/j.1365-246X.2008.04025.x.

Duputel, Z., L. Rivera, H. Kanamori, G. Hayes, B. Hirsorn, and S. Weinstein (2011), Real-time W phase inversion during the 2011 off the Pacific coast of Tohoku earthquake, *Earth Planets Space*, *63*, 535–539, doi:10.5047/eps.2011.05.032.

Dziewonski, A. M., and D. L. Anderson (1981), Preliminary reference Earth model, *Phys. Earth Planet. Inter.*, *25*, 297–356, doi:10.1016/0031-9201(81)90046-7.

Gilbert, F., and G. Backus (1968), Elastic-gravitational vibrations of a radially stratified sphere, in *Dynamics of Stratified Solids*, edited by G. Herrmann, pp. 82–95, Am. Soc. Mech. Eng., New York.

Han, S.-C., C. K. Shum, M. Bevis, C. Ji, and C. Kuo (2006), Crustal dilatation observed by GRACE after the 2004 Sumatra-Andaman earthquake, *Science*, *313*, 658–662, doi:10.1126/science.1128661.

Han, S.-C., J. Sauber, S. Luthcke, C. Ji, and F. Pollitz (2008), Implications of postseismic gravity change following the great 2004 Sumatra-Andaman earthquake from the regional harmonic analysis of GRACE intersatellite tracking data, *J. Geophys. Res.*, *113*, B11413, doi:10.1029/2008JB005705.

Han, S.-C., J. Sauber, and S. Luthcke (2010), Regional gravity decrease after the 2010 Maule (Chile) earthquake indicates large-scale mass redistribution, *Geophys. Res. Lett.*, *37*, L23307, doi:10.1029/2010GL045449.

Hayes, G. P. (2011), Rapid source characterization of the Mw 9.0 off the Pacific coast of Tohoku earthquake, *Earth Planets Space*, *63*, 529–534, doi:10.5047/eps.2011.05.012.

Heki, K., and K. Matsuo (2010), Coseismic gravity changes of the 2010 earthquake in central Chile from satellite gravimetry, *Geophys. Res. Lett.*, *37*, L24306, doi:10.1029/2010GL045335.

Kanamori, H., and J. W. Given (1981), Use of long-period surface waves for rapid determination of earthquake source parameters, *Phys. Earth Planet. Inter.*, *27*, 8–31, doi:10.1016/0031-9201(81)90083-2.

Lay, T., C. J. Ammon, H. Kanamori, L. Xue, and M. Kim (2011), Possible large near-trench slip during the 2011 Mw 9.0 off the Pacific coast of Tohoku earthquake, *Earth Planets Space*, *63*, 687–692, doi:10.5047/eps.2011.05.033.

Matsuo, K., and K. Heki (2011), Coseismic gravity changes of the 2011 Tohoku-Oki earthquake from satellite gravimetry, *Geophys. Res. Lett.*, *38*, L00G12, doi:10.1029/2011GL049018.

Melini, D., G. Spada, and A. Piersanti (2010), A sea level equation for seismic perturbations, *Geophys. J. Int.*, *180*, 88–100, doi:10.1111/j.1365-246X.2009.04412.x.

Miura, S., N. Takahashi, A. Nakanishi, T. Tsuru, S. Kodaira, and Y. Kaneda (2005), Structural characteristics off Miyagi forearc region, the Japan Trench seismogenic zone, deduced from a wide-angle reflection and refraction study, *Tectonophysics*, *407*, 165–188, doi:10.1016/j.tecto.2005.08.001.

Nettles, M., G. Ekstrom, and H. Koss (2011), Centroid–moment-tensor analysis of the 2011 off the Pacific coast of Tohoku earthquake and its larger foreshocks and aftershocks, *Earth Planets Space*, *63*, 519–523, doi:10.5047/eps.2011.06.009.

Okubo, S. (1992), Gravity and potential changes due to shear and tensile faults in a half-space, *J. Geophys. Res.*, *97*, 7137–7144, doi:10.1029/92JB00178.

Ozawa, S., T. Nishimura, H. Suito, T. Kobayashi, M. Tobita, and T. Imakiire (2011), Coseismic and postseismic slip of the 2011 magnitude-9 Tohoku-Oki earthquake, *Nature*, *475*, 373–376, doi:10.1038/nature10227.

Pollitz, F. (1997), Gravity anomaly from faulting on a layered spherical Earth with application to central Japan, *Phys. Earth Planet. Inter.*, *99*, 259–271, doi:10.1016/S0031-9201(96)03204-9.

Pollitz, F. F., R. Bürgmann, and P. Banerjee (2011), Geodetic slip model of the 2011 M9.0 Tohoku earthquake, *Geophys. Res. Lett.*, *38*, L00G08, doi:10.1029/2011GL048632.

Sato, M., et al. (2011), Displacement above the hypocenter of the 2011 Tohoku-Oki earthquake, *Science*, *332*, 1395, doi:10.1126/science.1207401.

Shao, G., X. Li, C. Ji, and T. Maeda (2011), Focal mechanism and slip history of 2011 Mw 9.1 off the Pacific coast of Tohoku earthquake, constrained with teleseismic body and surface waves, *Earth Planets Space*, *63*, 559–564, doi:10.5047/eps.2011.06.028.

Simons, M., et al. (2011), The 2011 magnitude 9.0 Tohoku-Oki earthquake: Mosaicking the megathrust from seconds to centuries, *Science*, *332*, 1421–1425, doi:10.1126/science.1206731.

Tapley, B. D., S. Bettadpur, J. Ries, P. Thompson, and M. Watkins (2004), GRACE measurements of mass variability in the Earth system, *Science*, *305*, 503–505, doi:10.1126/science.1099192.

U.S. Geological Survey (2011), USGS centroid moment solution: Near east coast of Honshu, Earthquake Hazards Program, Reston, Va., Japan [Available at http://earthquake.usgs.gov/earthquakes/eqinthenews/2011/usc0001xgp/neic_c0001xgp_cmt.php].

Watkins, M., et al. (2011), GRACE Follow-On Mission status, paper presented at GRACE Science Team Meeting, Austin, Tex., 8–10 Aug.

S.-C. Han and J. Sauber, Planetary Geodynamics Laboratory, NASA Goddard Space Flight Center, Code 698, Greenbelt, MD 20771, USA. (shin-chan.han@nasa.gov)

R. Riva, Faculty of Aerospace Engineering, Delft University of Technology, Kluyverweg 1, NL-2629 HS Delft, Netherlands.